

High-precision stellar parallaxes from *Hubble Space Telescope* fine guidance sensors†

G. Fritz Benedict and Barbara E. McArthur

McDonald Observatory, University of Texas, Austin, TX 78712, USA
email: fritz@astro.as.utexas.edu, mca@astro.as.utexas.edu

Abstract. We describe our experiences with on-orbit calibration of, and scientific observations with, the Fine Guidance Sensors (FGS), white-light interferometers aboard *Hubble Space Telescope*. Our original goal, 1 milliarcsecond precision parallaxes, has been exceeded on average by a factor of three, despite a mechanically noisy on-orbit environment, the necessary self-calibration of the FGS, and significant temporal changes in our instruments. To obtain accurate absolute parallaxes from these small fields of view ($3' \times 15'$) observations requires a significant amount of ancillary reference star information. These data also permit an independent estimate of interstellar absorption, critical in determining target absolute magnitudes, M_V , often the key result of a parallax program. With these techniques we and our collaborators have obtained absolute parallaxes for 21 astrophysically interesting objects. We briefly discuss a recent determination of the parallax of the Pleiades. *HST* routinely produces parallaxes with half the error of the best Hipparcos results, a precision that continues down to target $V = 15$. The FGS will remain a competitive astrometric tool for the generation of high-precision parallaxes until the advent of longer-baseline space-based interferometers (SIM), or the failure of some key *HST* component.

1. Introduction

We describe our experiences with on-orbit calibration and scientific observations with the Fine Guidance Sensors (FGS), white-light interferometers aboard *Hubble Space Telescope*. Our original goal, 1 milliarcsecond (mas) precision parallaxes, has been exceeded on average by a factor of three, but not without significant challenges. These included a mechanically noisy on-orbit environment, the self-calibration of an FGS (McArthur *et al.* 2002), and significant temporal changes in our instruments. Solutions included a denser set of drift check stars for each science observation, fine-tuning exposure times, overlapping field observations and analyses for calibration, and a continuing series of trend-monitoring observations.

To obtain accurate absolute parallaxes from these small field of view ($3' \times 15'$, shown in Fig. 1) differential astrometric observations requires a significant amount of ancillary reference star information. We employ combinations of visible (*BVRI*), near-infrared (*JHK*), and Washington-DDO (T_2 , M, DDO51) photometry, along with MK spectral types and luminosity classes from classification-dispersion spectra. These data also permit an independent estimate of interstellar absorption, critical in determining target absolute magnitudes, M_V , often a key result of the parallax effort (e.g., Benedict *et al.* 2002a).

† Based on observations made with the NASA/ESA Hubble Space Telescope, obtained at the Space Telescope Science Institute, which is operated by the Association of Universities for Research in Astronomy, Inc., under NASA contract NAS5-26555

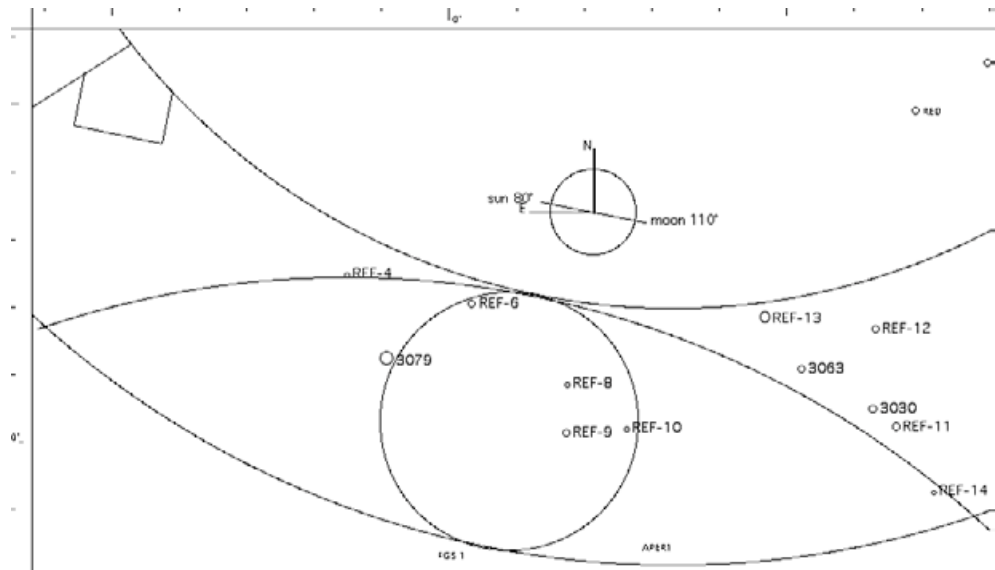


Figure 1. Field of regard of FGS 1 on the sky at the location of the Pleiades parallax targets 3030, 3063, and 3079 discussed in Section 5.1. Also shown are the reference stars, relative to which parallax and proper motion are obtained. The tick marks at top are spaced by $1'$.

2. The instrument and calibrations

Those with a deeper interest in the FGS instrument and calibration issues can find considerably more detail in Nelan & Makidon (2001) and McArthur *et al.* (2002), respectively.

2.1. Anatomy of an FGS

Each FGS is an interferometer. Interference takes place in a prism that has been sliced in half, had a quarter-wave retarding coating applied, and then reassembled. Most of the FGS consists of supporting optics used to feed the Koester's Prisms (top right, Fig. 2).

In particular the star selectors walk a $5''$ instantaneous field of view throughout the interferometer field of regard shown in Fig. 1. The output of each face of the Koester's Prism is measured by a PMT. These signals are combined

$$S = \frac{A - B}{A + B} \quad (2.1)$$

to form a signal, S , that is zero for waves exactly vertically incident on the Koester's Prism front face. Tilting the wavefront back and forth (equivalent to pointing the telescope slightly off, then on target, then slightly off to the other side) will generate a fringe pattern (Fig. 3). This technique of fringe scanning is often useful for resolved targets such as binary stars (Franz *et al.* 1998). For parallax work we obtain fringe tracking measurements. A series of measurements of the fringe zero-crossing position are obtained for each target and reference star. These are subjected to a median filter to produce a relative position within the FGS field of regard.

A perfect instrument would generate a perfectly symmetric fringe pattern. The significant spherical aberration of the as-built *HST* primary mirror, in the presence of internal FGS misalignments, produces a signature in the fringe which mimics coma. Coma causes decreased modulation and multiple peaks and valleys in a fringe. A replacement FGS installed in 1997 contains an articulated fold flat (FF3 in Fig. 2, center) that removes

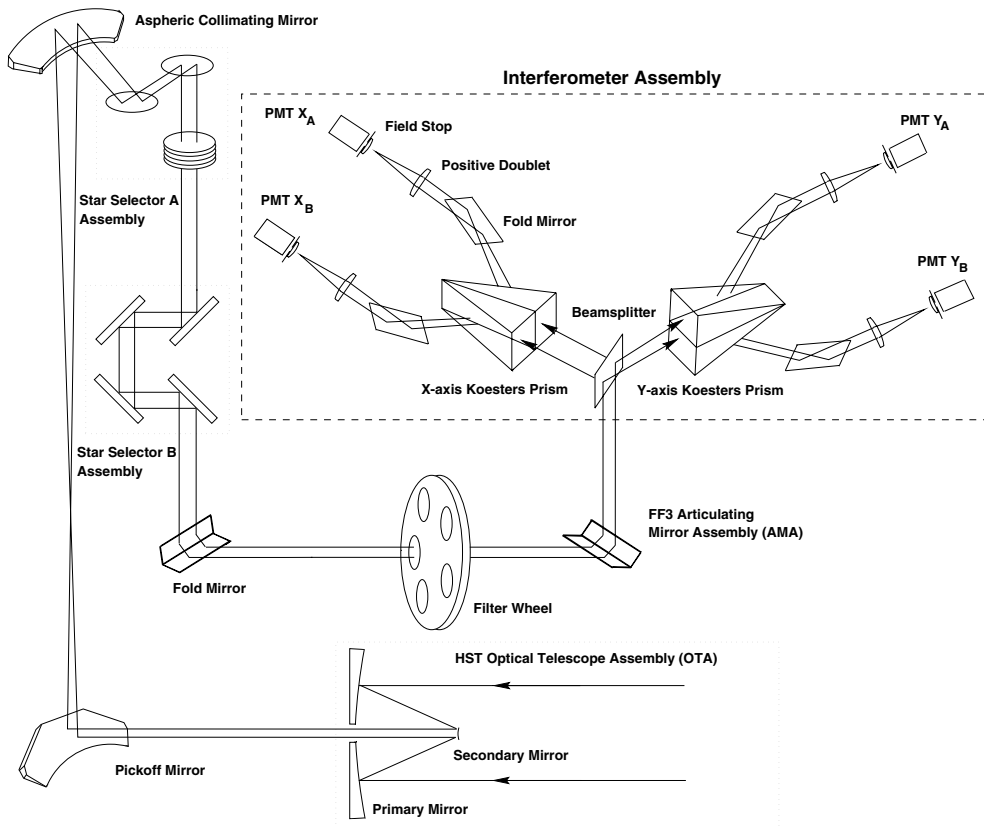


Figure 2. The optical layout of a Fine Guidance Sensor. We obtain fringe information for two orthogonal axes simultaneously.

most of the internal misalignments. This FGS (FGS 1r) produces nearly perfect fringes (Fig. 3), thus yielding far better fringe tracking and fringe scanning results.

2.2. The optical field angle distortion calibration

Optical distortions in the HST Ritchey-Chretien telescope and FGS combination have positional amplitudes in the focal plane exceeding $1''$. There was no existing star field with cataloged 1mas precision astrometry, our desired performance goal. Our solution was to use FGS to calibrate itself with multiple observations of a distant star field (M35). A distant field was required so that during the two-day duration of data acquisition, star positions would not change. We obtained these data in early 1993 for FGS 3 and in 2000 for FGS 1r and reduced them with overlapping plate techniques to solve for distortion coefficients and star positions simultaneously. As a result of this activity distortions are reduced to better than 2mas over much of the FGS field of regard. This model is called the Optical Field Angle Distortion (OFAD) calibration. Details can be found in McArthur *et al.* (2002). To date both FGS 3 and FGS 1r on *HST* have been calibrated

Once we have established a calibration we must maintain it: an FGS changes over months and years. For example, the FGS 3 graphite-epoxy optical bench was predicted to outgas for a period of time after the launch of *HST*, a process predicted to change the relative positions of optical components on the optical bench. As a consequence we revisit the M35 calibration field periodically to monitor these (scale-like) changes

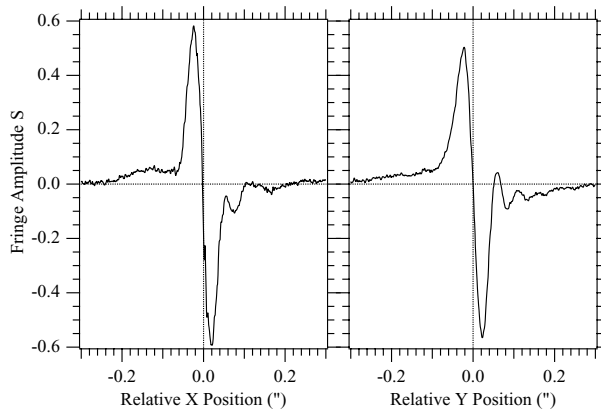


Figure 3. Fringe along the X and Y axes of FGS 1r. A series of fringe tracking measurements of the X and Y zero-crossing positions (the positions at which $S = 0$) are subjected to a median filter to produce a final X, Y position used for parallax work.

and other slowly varying non-linearities. This is the never-ending LTSTAB (Long-Term STABILITY) series. LTSTABs are required as long as it is desirable to do 1 mas precision astrometry with an FGS. The result of this series is to model and remove the slowly varying component of the OFAD, so that uncorrected distortions remain below 2 mas for center of an FGS. The character of these changes are generally monotonic with abrupt jumps in conjunction with HST servicing missions.

2.3. Lateral color

Because each FGS contains refractive elements (star selector A in Fig. 2), the position measured for a star can depend on its intrinsic color. This lateral color shift would be unimportant, as long as target and reference stars had similar color. However, this is certainly not the case for many of our science target stars (Table 1), hence our need for this calibration. For further details see Benedict *et al.* (1999).

2.4. Cross filter

The filter wheel in each FGS contains a neutral density filter with a 1% transmission (Nelan & Makidon 2001). This filter, designated FND5, provides 5 magnitudes of attenuation. This reduction of signal is required to obtain astrometry for stars that are brighter than $V = 8.5$, for which the count rate for the FGS PMTs would exceed the electronics capacity (Bradley *et al.* 1991). No filter has perfectly plane-parallel faces, an effect called filter wedge. Filter wedge introduces a slight shift in position when comparing an observation with the standard astrometry filter, F583W, with the FND5 filter. We required this latter filter to perform astrometry on RR Lyr, $V \sim 7.2$ and δ Cep, $V \sim 4$. To obtain milliarcsecond astrometry requires knowledge of the filter wedge effect to that precision or better.

Conceptually the calibration is simple. Observe in POS (fringe tracking) mode the same star with and without the FND5 filter and compare the positions. The shift so determined (Fig. 4) is then applied when comparing faint reference stars with bright science targets. The standard astrometry filter is F583W. As a consequence we actually measure differential filter wedge, because F583W is also a filter with non-parallel faces. Note that each filter is also a refractive element. Thus a star position will depend on the color of the star. This is an element of the lateral color effect discussed above.

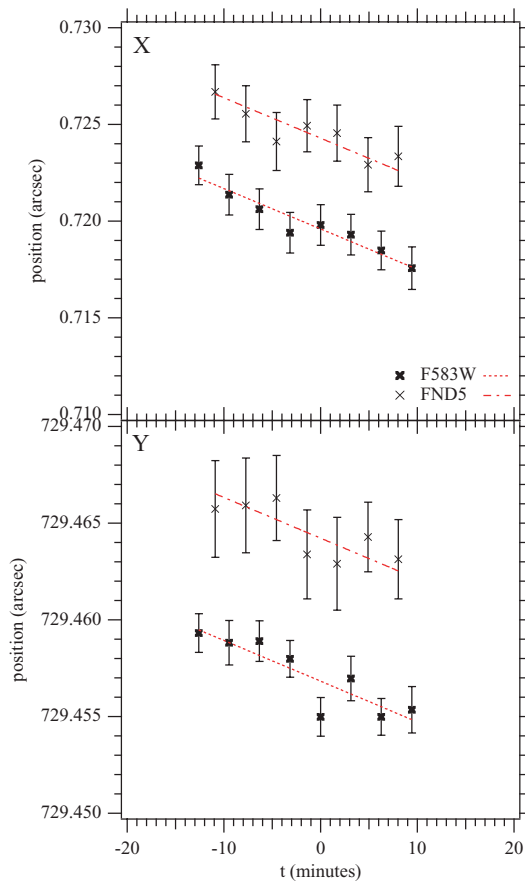


Figure 4. Cross filter calibration observations in 1998. Target is Uggren 69 in NGC 188. The plots show a shift in position between F583W and FND5 and typical intra-orbit drift in FGS 3.

3. Observations required for a parallax determination

3.1. Observing with an FGS

The issues summarized in this section are discussed at greater length in Benedict *et al.* (1998), particularly the intra-orbit observing strategies. A typical observation sequence has a duration of about 40 min and consists of a serial collection of from 10 to 30 time-series of positions sampled at 40 Hz. Each time series lasts from 30 to 300 s, depending on the target star brightness. We have identified sources of systematic and random position noise and discuss them from highest to lowest frequency.

We characterized the power spectrum of *HST* mechanical noise and determined that observing for 60 s or longer adequately sampled the frequency domain. A median filter was determined to abstract the best position (i.e., the median is a robust estimator for this system). The dispersion around the median provides an estimation of the observational error.

Over the course of an orbit guide stars autonomously drift as each FGS shifts slightly in its bay. Fig. 4 shows observations of a cross-filter calibration star over the span of 25 min. This behavior imposes additional overhead, reducing the time available within an orbit to do science. An observation set must contain multiple visits to two or more astrometric reference stars. Presuming no motion intrinsic to these stars over 40 min,

one determines drift and corrects the reference frame and target star for this drift. As a result we reduce the error budget contribution from drift to less than 1 mas.

Lastly, we arrange to observe our science targets and associated reference stars near times of maximum parallax factor. Some results have been secured with as few as six orbits over 1.5 yr. Typically we obtain around ten orbits over that same time span. The extra orbits result in better parallax precision. By bracketing times of maximum parallax factor with a pair of observations spaced by a week or so we also insure against rare *HST* equipment glitches. We also generally observe a few times at intermediate parallax factor to distinguish parallax from proper motion.

3.2. Ancillary observations

3.2.1. Spectrophotometric absolute parallaxes of the astrometric reference stars

Because the parallax determined by an FGS will be measured with respect to reference frame stars which have their own parallaxes, we must either apply a statistically derived correction from relative to absolute parallax (van Altena, Lee & Hoffleit 1995, hereafter YPC95) or, preferably, estimate the absolute parallaxes of the reference frame stars (e.g. Harrison *et al.* 1999). With colors, spectral type, and luminosity class for a star one can estimate the absolute magnitude, M_V , and V -band absorption, A_V . The absolute parallax is then,

$$\pi_{abs} = 10^{-(V-M_V+5-A_V)/5} \quad (3.1)$$

The luminosity class is generally more difficult to determine than the spectral type (temperature class). However, the derived absolute magnitudes are critically dependent on the luminosity class. To confirm the luminosity classes we generally employ the technique used by Majewski *et al.* (2000) to discriminate between giants and dwarfs for stars later than $\sim G5$, an approach whose theoretical underpinnings are discussed by Paltoglou & Bell (1994). The boundary between giants and dwarfs is ‘fuzzy’ and complicated by the photometric transition from dwarfs to giants through subgiants. This soft boundary is readily apparent in figure 14 of Majewski *et al.* (2000). However, objects above the boundary are statistically more likely to be giants than objects just below.

- Photometry – Our band-passes for reference star photometry include: *BVRI*, *JHK* (from 2MASS[†]), and Washington/DDO filters M, 51, and T₂ (obtained at McDonald Observatory with the 0.8-m Prime Focus Camera). We transform the 2MASS *JHK* to the Bessell (1988) system, using the transformations provided in Carpenter (2001).

- Spectroscopy – The spectra from which we estimated spectral type and luminosity class come from several sources. Classifications are obtained by a combination of template matching and line ratios, often by two independent co-investigators.

- Interstellar Extinction – To determine interstellar extinction we first plot our reference stars on several color-color diagrams. A comparison of the relationships between spectral type and intrinsic color against measured colors provides an estimate of reddening. Fig. 5 contains $V - R$ vs $V - K$ and $V - I$ vs $V - K$ color-color diagrams and reddening vectors for our RR Lyr campaign (Benedict *et al.* 2002a). Also plotted are mappings between spectral type and luminosity class V and III from Bessell & Brett (1988) and Cox (2000, hereafter AQ00), again with reddening vectors and the loci of luminosity classes V and III stars. Fig. 5, along with the estimated spectral types, provides measures of the reddening for each reference star.

Assuming an $R = 3.1$ galactic reddening law (Savage & Mathis 1977), we derive A_V values by comparing the measured colors with intrinsic $V - R$, $V - I$, $J - K$, and

[†] The Two Micron All Sky Survey is a joint project of the University of Massachusetts and the Infrared Processing and Analysis Center/California Institute of Technology

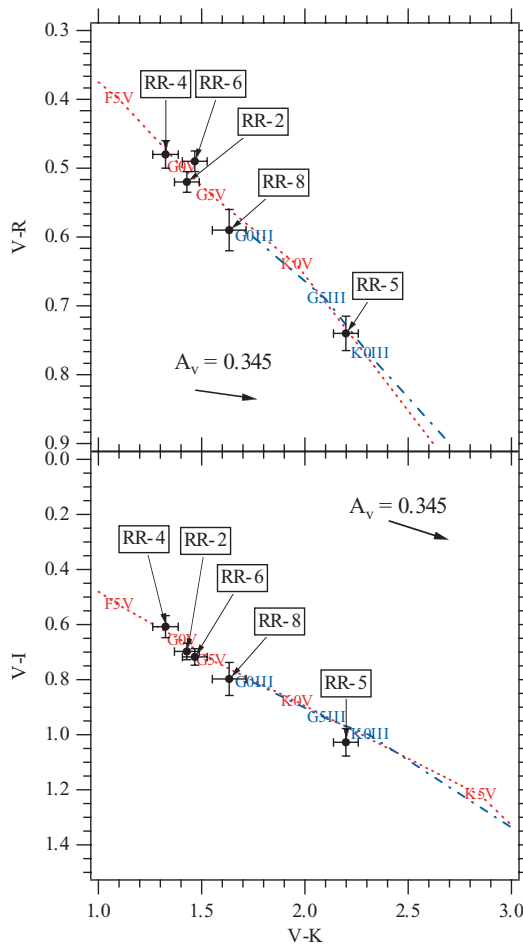


Figure 5. $V - R$ vs $V - K$ and $V - I$ vs $V - K$ color-color diagrams and reddening vectors, photometry used for our RR Lyr campaign (Benedict *et al.* 2002a).

$V - K$ colors from Bessell & Brett (1988) and AQ00. Specifically, we estimate A_V from four different ratios, each derived from the Savage & Mathis (1977) reddening law: $A_V/E(V - R) = 4.83$; $A_V/E(V - K) = 1.05$; $A_V/E(J - K) = 5.80$; and $A_V/E(V - I) = 2.26$. For some fields colors and spectral types are inconsistent with a field-wide average $\langle A_V \rangle$. This was the case for the δ Cep field, where we ultimately adopted the reddening of the most proximate reference star as the target reddening (Benedict *et al.* 2002b).

3.2.2. The inclusion of prior knowledge

When possible, prior knowledge bearing on the determination of target parallax is included in our modeling process. This information passes to the model as observations with errors which weight their influence on the final outcome. This approach allows us to incorporate *any* measurements relevant to our investigation. Here are two examples of this quasi-Bayesian approach.

- In determining the parallax of δ Cep we had prior knowledge that reference star DC-2 was thought to be physically associated with δ Cep. This association was established through common proper motion. Also de Zeeuw *et al.* (1999) include both δ Cep and DC-2 in the Cep OB6 association. We constrained the difference in parallax between δ Cep

and DC-2, using our prior knowledge of their association. From de Zeeuw *et al.* (1999) we estimated that the 1σ dispersion in Galactic longitude for the OB association thought to contain both δ Cep and DC-2 is 3° . One can therefore infer that the 1σ dispersion in distance in this group is $3^\circ/\text{radian} \sim 5\%$. Hence, the 1σ dispersion in the parallax difference between two group members (e.g. DC-2 and δ Cep) is

$$\Delta\pi = 5\% \times \sqrt{2} \times 3.7 \text{ mas} = 0.26 \text{ mas} \quad (3.2)$$

where we have here adopted the mean parallax of Cep OB6, $\langle\pi\rangle = 3.7 \text{ mas}$, from de Zeeuw *et al.* (1999). The assumed zero parallax difference between δ Cep and DC-2 becomes an observation with an associated error ($\Delta\pi$) fed to our model, an observation used to estimate the parallax difference between the two stars, while solving for the parallax of δ Cep.

- The reference star spectrophotometric absolute parallaxes are input as observations with errors, not as hardwired quantities known to infinite precision. The lateral color and cross-filter calibrations, as well as $B - V$ color indices, are entered into the model as observations with associated errors. We now also introduce proper motion data from UCAC2 (Zacharias *et al.* 2003) with typical input errors 5 mas in each coordinate.

4. The astrometric model

With the positions measured by an FGS we determine the scale, rotation, and offset “plate constants” relative to an arbitrarily adopted constraint epoch (the so-called “master plate”) for each observation set (the data acquired at each epoch). Depending on reference frame characteristics (number and distribution of reference stars), we employ models with four to eight parameters (e.g., McArthur *et al.* 2001; Benedict *et al.* 2003) for those observations. In some of our earliest work we determined the plate parameters from reference star data only, then applied them as constants to obtain the parallax and proper motion of the science target. Usually we determine the plate parameters and the parallax and proper motion of the science target and reference stars simultaneously. Typically the reference stars have color indices that differ from the science target, and we apply the corrections for lateral color discussed in Benedict *et al.* (1999).

For all our astrometric analyses, we employ GaussFit (Jefferys *et al.* 1987) to minimize χ^2 . The solved equations of condition are typically:

$$x' = x + lcx(B - V) \quad (4.1)$$

$$y' = y + lcy(B - V) \quad (4.2)$$

and

$$\xi = Ax' + By' + C + R_x(x'^2 + y'^2) - \mu_x\Delta t - P_\alpha\pi_x \quad (4.3)$$

$$\eta = -Bx' + Ay' + F + R_y(x'^2 + y'^2) - \mu_y\Delta t - P_\delta\pi_y \quad (4.4)$$

or

$$\xi = Ax' + By' + C - \mu_x\Delta t - P_\alpha\pi_x \quad (4.5)$$

$$\eta = Dx' + Ey' + F - \mu_y\Delta t - P_\delta\pi_y \quad (4.6)$$

where x and y are the measured coordinates from *HST*; lcx and lcy are the lateral color corrections; and $B - V$ are the $B - V$ colors of each star. A, B, D, and E are scale and rotation plate constants, C and F are offsets; R_x and R_y are radial terms; μ_x and μ_y are proper motions; Δt is the epoch difference from the mean epoch; P_α and P_δ are parallax

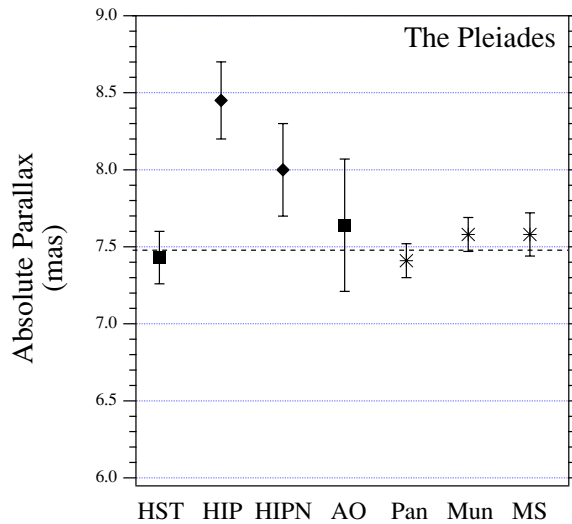


Figure 6. Absolute parallax determinations for the Pleiades. We compare astrometric parallax results (filled squares) from *HST* and Allegheny Observatory (AO, Gatewood *et al.* 2000) with Hipparcos (filled diamonds), both an older result (HIP, van Leeuwen 1999) and a very recent re-determination (HIPN, van Leeuwen 2004). Pan *et al.* (2004) have derived a dynamical parallax from long baseline interferometry of the binary star, Atlas. Munari *et al.* (2004) have determined a dynamical parallax using an eclipsing SB2 binary. MS denotes a parallax derived from main-sequence fitting (Pinsonneault *et al.* 1998). The horizontal dashed line is the weighted average of the *HST*, Pan, Munari, and AO measures, $\langle \pi_{abs} \rangle = 7.49 \pm 0.07$ mas.

factors; and π_x and π_y are the parallaxes in x and y. See Benedict *et al.* (2002b) for a model that includes cross-filter corrections. We obtain the parallax factors from a JPL Earth orbit predictor (Standish 1990), upgraded to version DE405. Before the existence of a reliable source for proper motions, we imposed the constraint that the reference star proper motions are random in direction by forcing their sum in x and y to be zero, $\sum \mu_x = \sum \mu_y = 0$. Orientation to the sky is obtained from ground-based astrometry (e.g., USNO-A2.0 catalog, Monet 1998) with uncertainties in the field orientation $\pm 0^\circ 05$.

The solution process is allowed to adjust any input parameter by an amount depending on its variance to find the ‘best’ solution. These input parameters include previously measured colors, proper motions, reference star parallaxes estimated from spectrophotometry, the orientation of the reference plate to RA and Dec, and the lateral color and cross filter corrections.

5. Results

The choice of *HST* astrometry science targets is rightly determined by what can be done from the ground. The unique capabilities of *HST* must remain reserved for projects demanding them. It is by now clear that a significant investment of time and effort is required to obtain a parallax from FGS data. However, this investment guarantees parallax precision at or below 0.5 mas for objects as faint as $V = 15$.

With these techniques we have determined more precise absolute magnitudes for the distance-scale standards, RR Lyr and δ Cep. We have obtained absolute magnitudes and radii for two hot white dwarf stars, Feige 24 and the central star of the planetary nebula NGC 6853. We have generated precise distances with which to constrain theories of

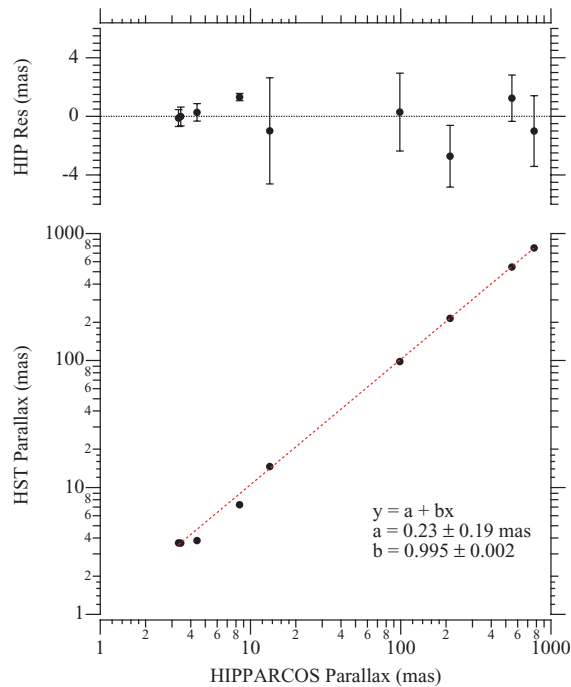


Figure 7. Bottom: *HST* absolute parallax determinations compared with Hipparcos for targets in common listed in Table 1. Top: The Hipparcos residuals to the dotted error-weighted impartial regression line that excludes the Pleiades. The error bars on the residuals are Hipparcos Catalog 1- σ errors.

the star-star interactions evidenced by cataclysmic variables (TV Col, RW Aur, WZ Sge, YZ Cnc, U Gem, SS Aur, SS Cyg, RU Peg, and EX Hya). Other investigations have treated the parallax as a nuisance parameter that must be removed with exquisite precision to determine the perturbation due to a planetary mass companion (Gl 876b), or to generate precise binary star orbital elements and component masses (Gl 791.2, Wolf 1062), from orbits whose dimensions on the sky are smaller than the typical seeing at an excellent ground-based observing site. Table 1 lists all objects for which we have derived parallaxes, including our soon to be published result for the Pleiades, which we now discuss in more detail.

5.1. A parallax for the Pleiades

We have recently completed a study of three members of the Pleiades. A full account of this study will appear shortly (Soderblom *et al.* 2004). Our original intent was to determine orbital parameters for several binaries thought to belong to the Pleiades. After realizing that FGS 1r could not adequately resolve these binaries, this dynamical parallax experiment changed to a standard parallax program for the three Pleiads in the field. Because of this the timing of the observation illustrated in Fig. 1 was not optimal for maximum parallax factor, having a Sun-target field separation of 80°, shown on the compass rose.

Six sets of astrometric data were acquired with *HST*, spanning 3.51 yr, for a total of 135 measurements of the three Pleiads (stars 3030, 3063, and 3179 in Fig. 1) and nine reference stars (see Fig. 1). Spectral types and luminosity classes were estimated from classification dispersion spectra. This information, with JHK photometry from 2MASS and *V* photometry from the FGS yielded reference frame absolute parallaxes through

Table 1. *HST* and Hipparcos Absolute Parallaxes. The last six parallaxes were obtained with FGS 1r. All others were obtained with FGS 3.

Object	<i>HST</i> mas	Hip mas	<i>HST</i> Reference
Prox Cen	769.7 ± 0.3	772.3 ± 2.4	Benedict <i>et al.</i> 1999
Barnard's Star	545.5 ± 0.3	549.3 ± 1.58	Benedict <i>et al.</i> 1999
U Gem	9.96 ± 0.37		Harrison <i>et al.</i> 1999
SS Aur	5.99 ± 0.33		Harrison <i>et al.</i> 1999
SS Cyg	6.06 ± 0.44		Harrison <i>et al.</i> 1999
RW Tri	2.93 ± 0.33		McArthur <i>et al.</i> 1999
Feige 24	14.6 ± 0.4	13.44 ± 3.62	Benedict <i>et al.</i> 2000a
Gl 791.2	113.1 ± 0.3		Benedict <i>et al.</i> 2000b
Wolf 1062	98.0 ± 0.4	98.56 ± 2.66	Benedict <i>et al.</i> 2001
TV Col	2.70 ± 0.11		McArthur <i>et al.</i> 2001
RR Lyr	3.60 ± 0.20	4.38 ± 0.59	Benedict <i>et al.</i> 2002a
δ Cep	3.66 ± 0.15	3.32 ± 0.58	Benedict <i>et al.</i> 2002b
HD 213307	3.65 ± 0.15	3.43 ± 0.64	Benedict <i>et al.</i> 2002b
Gl 876	214.6 ± 0.2	212.7 ± 2.1	Benedict <i>et al.</i> 2002c
NGC 6853	2.10 ± 0.48		Benedict <i>et al.</i> 2003
Ex Hya	15.50 ± 0.29		Beuermann <i>et al.</i> 2003
V1223 Sgr	1.96 ± 0.18		Beuermann <i>et al.</i> 2004
RU Peg	3.55 ± 0.26		Harrison <i>et al.</i> 2004
WZ Sge	22.97 ± 0.15		Harrison <i>et al.</i> 2004
YZ Cnc	3.34 ± 0.45		Harrison <i>et al.</i> 2004
Pleiades	7.43 ± 0.17	8.45 ± 0.25	Soderblom <i>et al.</i> 2004

equation 3.1. Reference star proper motions were obtained from UCAC2. A final piece of prior knowledge (Section 3.2.2) came from the assumption that our targets were in fact members of the Pleiades. This assumption generates an ‘observation’ asserting that the difference in parallax between our Pleiades member target stars is zero. The error associated with this ‘observation’ comes from the $1\text{-}\sigma$ angular extent of the Pleiades (1° , from Adams *et al.* 2001) and an assumption of spherical symmetry. From equation 3.2, we assert that the 1σ dispersion in distance in this group is $1^\circ/\text{radian} = 1.7\%$. Hence, the 1σ dispersion in the parallax difference between Pleiades members is $\Delta\pi = 0.20$ mas, where we have here temporarily adopted a parallax of the Pleiades, $\langle\pi\rangle = 7.7$ mas. The parallax dispersion among targets 3030, 3179, and 3063 becomes an observation with associated error fed to our model, an observation used to estimate the parallax dispersion among the three stars, while solving for their parallaxes. Neither loosening the cluster $1\text{-}\sigma$ dispersion to 2° ($\Delta\pi = 0.38$ mas) nor adopting the HIPPARCOS parallax in equation 3.2 had any effect on the final average parallax.

Note that the priors did not include any previous direct observations of the parallax of the Pleiades. Our model used equations 4.1, 4.2, 4.5 and 4.6. We obtained an average parallax for the three Pleiades members $\pi_{abs} = 7.43 \pm 0.17$ mas. This result continues the trend of resolving the dispute between the main sequence fitting and the Hipparcos distance moduli in favor of main sequence fitting (Munari *et al.* 2004, Pan *et al.* 2004, Gatewood *et al.* 2000). Fig. 6 summarizes absolute parallax determinations for the Pleiades. Note that the very recent re-determination from Hipparcos raw data (van Leeuwen 2004, these proceedings) moves the parallax closer to our result and the average of the other determinations.

5.2. *HST* parallax accuracy

To assess our accuracy, or external error, we must compare our parallaxes with results from independent measurements. Table 1 includes an Hipparcos parallax, when available. We plot all parallaxes obtained with an FGS against those obtained by Hipparcos (Fig. 7). The dashed line is a weighted regression that takes into account errors in both input data sets and excludes the Pleiades. For this fit we obtain a reduced $\chi^2 = 0.265$. Including the Pleiades, we obtain a significantly poorer fit with reduced $\chi^2 = 0.551$, again, indicating a problem with the Hipparcos Pleiades parallax.

The regression seen in Fig. 7 indicates a 2.5σ scale difference between the Hipparcos and *HST* results. Measured proper motions provide an argument against the reality of this scale difference. Because it is desirable to reduce the impact of proper motion errors on an *HST* – Hipparcos comparison, we consider only two of the objects in Table 1, Proxima Cen and Barnard's Star. They have proper motion vector lengths exceeding 3800 mas yr^{-1} . Comparing *HST* with Hipparcos, the average difference between these proper motion vectors is -0.01% , indicating a negligible scale difference.

Presently continuing parallax investigations include a determination of the Cepheid period-luminosity relation through precise parallaxes of eleven Cepheids. We have nearly completed several more extrasolar planet mass determinations by removing the signature of parallax from observations of ν And and ϵ Eri. Finally we will assist in tightening up the lower main sequence mass-luminosity relation through astrometry of low mass binaries. In this case the parallax bears on the component masses and must be removed from orbital motion.

Acknowledgements

We thank our many co-investigators for their cheerful collaboration over the years: Klaus Beuermann, Art Bradley, Ray Duncombe, Otto Franz, Thierry Forveille, Geoff Marcy, Larry Fredrick, Paul Groot, Tom Harrison, Paul Hemenway, Todd Henry, Bill Jefferys, Ed Nelan, Ricky Patterson, Pete Shelus, Dave Soderblom, Bill Spiesman, Darrell Story, Bill van Altena, Qiangguo Wang, Larry Wasserman, and Art Whipple. We would like to acknowledge the support of Guaranteed Time Observer grants GO-06036, 06764, 06875, 06877, 06879, and 06880; and Guest Observer grants GO-08102, 08335, 08618, 09089, 09167, 09168, 09879; all administered through the Space Telescope Science Institute, which is operated by AURA, Inc., under NASA contract NAS5-26555. We are beholden to the support scientists at STScI who have assisted us over the years, especially Denise Taylor. Lastly we thank the many people in Danbury CT who have surfed the waves of change (once Perkin-Elmer, then Hughes Aerospace, then Raytheon, now Goodrich) and continue to support the FGS, especially Linda Abramowicz-Reed.

References

- Adams, J. D., Stauffer, J. R., Monet, D. G., Skrutskie, M. F., & Beichman, C. A. 2001, *Astron. J.*, **121**, 2053
- Benedict, G. F., McArthur, B., Nelan, E. P., Jefferys, W. H., Franz, O. G., Wasserman, L. H., Story, D. B., Shelus, P. J., Whipple, A. L., Bradley, A. J., Duncombe, R. L., Wang, Q., Hemenway, P. D., van Altena, W. F., & Fredrick, L. W. 1998, *Proc. S.P.I.E.*, **3350**, 229
- Benedict, G. F., McArthur, B., Chappell, D. W., Nelan, E., Jefferys, W. H., van Altena, W., Lee, J., Cornell, D., Shelus, P. J., Hemenway, P. D., Franz, O. G., Wasserman, L. H., Duncombe, R. L., Story, D., Whipple, A., & Fredrick, L. W. 1999, *Astron. J.*, **118**, 1086
- Benedict, G. F., McArthur, B. E., Franz, O. G., Wasserman, L. H., Nelan, E., Lee, J., Fredrick, L. W., Jefferys, W. H., van Altena, W., Robinson, E. L., Spiesman, W. J., Shelus, P. J.,

- Hemenway, P. D., Duncombe, R. L., Story, D., Whipple, A. L., & Bradley, A. 2000a, *Astron. J.*, **119**, 2382
- Benedict, G. F., McArthur, B. E., Franz, O. G., Wasserman, L. H., & Henry, T. J. 2000b, *Astron. J.*, **120**, 1106
- Benedict, G. F., McArthur, B. E., Fredrick, L. W., Harrison, T. E., Lee, J., Slesnick, C. L., Rhee, J., Patterson, R. J., Nelan, E., Jefferys, W. H., van Altena, W., Shelus, P. J., Franz, O. G., Wasserman, L. H., Hemenway, P. D., Duncombe, R. L., Story, D., Whipple, A. L., & Bradley, A. J. 2002a, *Astron. J.*, **123**, 473
- Benedict, G. F., McArthur, B. E., Fredrick, L. W., Harrison, T. E., Slesnick, C. L., Rhee, J., Patterson, R. J., Skrutskie, M. F., Franz, O. G., Wasserman, L. H., Jefferys, W. H., Nelan, E., van Altena, W., Shelus, P. J., Hemenway, P. D., Duncombe, R. L., Story, D., Whipple, A. L., & Bradley, A. J. 2002b, *Astron. J.*, **124**, 1695
- Benedict, G. F., McArthur, B. E., Forveille, T., Delfosse, X., Nelan, E., Butler, R. P., Spiesman, W., Marcy, G., Goldman, B., Perrier, C., Jefferys, W. H., & Mayor, M. 2002c, *Astrophys. J. Lett*, **581**, L115
- Benedict, G. F., McArthur, B. E., Fredrick, L. W., Harrison, T. E., Skrutskie, M. F., Slesnick, C. L., Rhee, J., Patterson, R. J., Nelan, E., Jefferys, W. H., van Altena, W., Montemayor, T., Shelus, P. J., Franz, O. G., Wasserman, L. H., Hemenway, P. D., Duncombe, R. L., Story, D., Whipple, A. L., & Bradley, A. J. 2003, *Astron. J.*, **126**, 2549
- Bessell, M. S. & Brett, J. M. 1988, *Pub Astron. Soc. Pacific*, **100**, 1134
- Beuermann, K., Harrison, T. E., McArthur, B. E., Benedict, G. F., & Gänsicke, B. T. 2003, *Astron. & Astrophys.*, **412**, 821
- Beuermann, K., Harrison, T. E., McArthur, B. E., Benedict, G. F., & Gänsicke, B. T. 2004, *Astron. & Astrophys.*, **419**, 291
- Bradley, A., Abramowicz-Reed, L., Story, D., Benedict, G. & Jefferys, W. 1991, *Pub Astron. Soc. Pacific*, **103**, 317
- Carpenter, J. M. 2001, *Astron. J.*, **121**, 2851
- Cox, A. N. 2000, Allen's astrophysical quantities, 4th ed. Publisher: New York: AIP Press, Springer, 2000. Edited by Arthur N. Cox. (AQ00)
- de Zeeuw, P. T., Hoogerwerf, R., de Bruijne, J. H. J., Brown, A. G. A., & Blaauw, A. 1999, *Astron. J.*, **117**, 354
- Franz, O. G., Henry, T. J., Wasserman, L. H., Benedict, G. F., Ianna, P. A., Kirkpatrick, J. D., McCarthy, D. W., Bradley, A. J., Duncombe, R. L., Fredrick, L. W., Hemenway, P. D., Jefferys, W. H., McArthur, B. E., Nelan, E. P., Shelus, P. J., Story, D. B., van Altena, W. F., & Whipple, A. L. 1998, *Astron. J.*, **116**, 1432
- Gatewood, G., de Jonge, J. K., & Han, I. 2000, *Astrophys. J.*, **533**, 938
- Hanson, R. B. 1979, *Mon. Not. Royal Astron. Soc.*, **186**, 87
- Harrison, T. E., McNamara, B. J., Szkody, P., McArthur, B. E., Benedict, G. F., Klemola, A. R., & Gilliland, R. L. 1999, *Astrophys. J. Lett*, **515**, L93
- Harrison, T. E., Johnson, J. J., McArthur, B. E., Benedict, G. F., Szkody, P., Howell, S. B., & Gelino, D. M. 2004, *Astron. J.*, **127**, 460
- Jefferys, W., Fitzpatrick, J., & McArthur, B. 1987, *Celest. Mech.*, **41**, 39.
- Majewski, S. R., Ostheimer, J. C., Kunkel, W. E., & Patterson, R. J. 2000, *Astron. J.*, **120**, 2550
- McArthur, B., Benedict, G. F., Jefferys, W. H., & Nelan, E. 2002, The 2002 HST Calibration Workshop : Hubble after the Installation of the ACS and the NICMOS Cooling System, Proceedings of a Workshop held at the Space Telescope Science Institute, Baltimore, Maryland, October 17 and 18, 2002. Edited by Santiago Arribas, Anton Koekemoer, and Brad Whitmore. Baltimore, MD: Space Telescope Science Institute, 2002, p.373
- McArthur, B. E. *et al.* 2001, *Astrophys. J.*, **560**, 907
- McArthur, B. E., Benedict, G. F., Lee, J., Lu, C.-L., van Altena, W. F., Deliyannis, C. P., Girard, T., Fredrick, L. W., Nelan, E., Duncombe, R. L., Hemenway, P. D., Jefferys, W. H., Shelus, P. J., Franz, O. G., & Wasserman, L. H. 1999, *Astrophys. J. Lett*, **520**, L59
- Monet, D. G. 1998, American Astronomical Society Meeting, 193, 112.003
- Munari, U., Dallaporta, S., Siviero, A., Soubiran, C., Fiorucci, M., & Girard, P. 2004, *Astron. & Astrophys.*, **418**, L31

- Nelan, E. & Makidon, R. 2001, *Fine Guidance Sensor Instrument Handbook* (version 10; Baltimore: STScI)
- Paltoglou, G. & Bell, R. A. 1994, *Mon. Not. Royal Astron. Soc.*, **268**, 793
- Pan, X., Shao, M., & Kulkarni, S. R. 2004, *Nature*, **427**, 326
- Pinsonneault, M. H., Stauffer, J., Soderblom, D. R., King, J. R., & Hanson, R. B. 1998, *Astrophys. J.*, **504**, 17
- Savage, B. D. & Mathis, J. S. 1979, *Ann Rev. Astron. & Astrophys.*, **17**, 73
- Soderblom, D., Benedict, G. McArthur. B. Nelan, E. *et al.* 2004, in preparation
- Standish, E. M., Jr. 1990, *Astron. & Astrophys.*, **233**, 252
- van Altena, W. F., Lee, J. T., & Hoffleit, E. D. 1995, *Yale Parallax Catalog* (4th ed. ; New Haven, CT: Yale Univ. Obs.) (YPC95)
- van Leeuwen, F. 1999, *Astron. & Astrophys.*, **341**, L71
- van Leeuwen, F. , 2004, *Transit of Venus: New Views of the Solar System and Galaxy*, Proceedings IAU Colloquium No. 196, D.W. Kurtz & G.E. Bromage, eds. in press
- Zacharias, N., Urban, S. E., Zacharias, M. I., Wycoff, G. L., Hall, D. M., Germain, M. E., Holdenried, E. R., & Winter, L. 2003, *VizieR Online Data Catalog*, 1289

Discussion

SUZANNE DÉBARBAT: Where did the idea for astrometry with the Hubble Space Telescope originate?

FRITZ BENEDICT: Why was there any place for astrometry on Hubble space telescope? Because they needed to point the damn thing! They needed to point it and they needed to hold it on target. The fine-guidance sensors' primary job was to acquire guide stars on either side of the targets so that they could take the pretty pictures. And if the fine-guidance sensors can hold things to within 2, 3, 4, 5, 6 milli-arcseconds, that's well smaller than the pixel size of the camera and you get those beautiful pictures. To echo Dave [Monet]: astrometry was "free". It wasn't a \$100 million; it wasn't even \$10 million. I will grant you it was probably about \$5 million over the 25 years ... [slight pause with a sense of wonder at this length of time] ... that I've been working on this project.



Fritz "Hook-em Horns" Benedict